CEMA를 이용한 자발화 한계근처 난류 비예혼합 수소 화염의 직접수치모사 연구

김승욱* · Jacqueline H. Chen** · 유춘상*†

A DNS Study of Stabilization Mechanisms of Turbulent Lifted Hydrogen Jet Flames with CEMA

Seung Ook Kim*, Jacqueline H. Chen**, Chun Sang Yoo*†

ABSTRACT

The characteristics of turbulent lifted non-premixed hydrogen jet flames under various coflow conditions have widely been investigated due to their relevance to practical applications. Three 3-D direct numerical simulations of turbulent lifted hydrogen/air jet flames in heated coflows near auto-ignition limit are performed to examine the stabilization mechanisms and flame structure of turbulent lifted jet flames. Chemical explosive mode analysis (CEMA) reveals the important variables and reactions for stabilizing the lifted flames.

Key Words: DNS, H_2 jet flames, stabilization mechanism

Three different direct numerical simulations (DNSs) of spatially-developing turbulent lifted jet flames were performed in a 3-D slot-burner configuration. Fuel issues from a central jet, which consists of 65% hydrogen and 35% nitrogen by volume at an inlet temperature of T_j=400K. The central jet is surrounded on either side by co-flowing heated air streams at three different temperatures of T_c = 750 (Case L), 850 (Case M), and 950 K (Case H) and atmospheric pressure. The fuel jet and coflow velocities are specified as U_j = 240 m/s and and U_c = 2 m/s, respectively. The fuel jet width, H, is 2 mm such that the jet Reynolds number, $Re_j = (U_j H/\nu)$, is approximately 8000. The computational domain is $15H \times 20H \times 3H$ in the streamwise, x, transverse, y, and spanwise, z, directions with 2000×1600×400 grid points. A uniform grid spacing of 15 μm is used in the x- and z-directions, while an algebraically stretched mesh is used in the y-direction as in [1].

The compressible Navier-Stokes, species continuity, and total energy equations were solved using the Sandia DNS code, S3D, with a 4th-order Runge-Kutta method for time integration and an 8th-order central differencing scheme for spatial discretization. A detailed hydrogen/air kinetic mechanism was adopted for DNSs [2]. Improved nonreflecting inflow/outflow boundary conditions [3,4] were used in the x- and y-directions and periodic boundary conditions were applied in the homogeneous z-direction. Based on the fuel jet velocity and the streamwise domain length, a flow-through time, $\tau_j = L_x / U_j$, is 0.125 ms. To obtain a stationary lifted flame while reducing computational cost, a simulation with a grid resolution of 40 μm was first performed until the flame attained statistical stationarity. The solutions from the simulation were then mapped onto a finer grid of 15 μm and used as an initial condition for the fully resolved simulations. Note that the steady lift-off heights are found to be approximately $\overline{h}_H/H$ =2.4, $\overline{h}_M/H$=4.0, and $\overline{h}_L/H$=5.3. Figure 1 shows 3-D volume-rendering of the mass fraction of OH and HO_2 at t/τ_j=2.0.

Chemical explosive mode analysis (CEMA) is adopted to further identify the characteristics of the lifted flamebases [5,7].

* 유니스트 기계공학과
** Combustion Research Facility, Sandia National Laboratories
† 연락저자, csyoo@unist.ac.kr
TEL : (052)217-2322 FAX : (052)217-2309

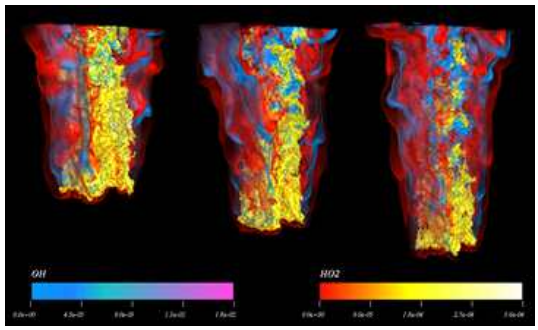

Figure 1. 3-D volume rendering of OH and HO_2 mass fractions of turbulent lifted hydrogen jet flames for Cases L, M, and H (from left to right)

CEMA is briefly introduced here and for more details of it, refer to [5,6]. The differential equations of a typical reacting flow can be described in discretized form as:

$$\frac{D\mathbf{y}}{Dt} = \mathbf{g}(\mathbf{y}) = \boldsymbol{\omega}(\mathbf{y}) + \mathbf{s}(\mathbf{y}),$$

where D/Dt is the material derivative and $\mathbf{y}$ represents the solution vector of species concentrations and temperature. The chemical source term is denoted as $\boldsymbol{\omega}$, while all non-chemical source terms such as diffusion in flames and homogeneous mixing term in stirred reactors are represented by $\mathbf{s}$.

CEM is defined as a chemical mode of which real part of the eigenvalue, λ_e, is positive. CEM represents the reciprocal chemical time scale of a local mixture and as such, the existence of CEM implies that the corresponding mixture is explosive in nature. It is, therefore, apt to auto-ignite when the mixture resides in a lossless environment with negligible $\mathbf{s}$. CEM is an intrinsic characteristic of ignitable mixtures.

In nonpremixed turbulent flames, the loss of heat and radicals can be characterized by the mixing or scalar dissipation rate, χ, which is defined by $\chi = 2D|\nabla\xi|^2$, where D is local thermal diffusivity. The competition between the CEMs and the loses can approximately be quantified by a Damköhler number defined by $Da_c = \lambda_e \cdot \chi^{-1}$. Note that mixture with $Da_c \gg 1$ indicates a dominant CEM which will be likely to result in actual ignition; otherwise ignition may be suppressed by the losses.

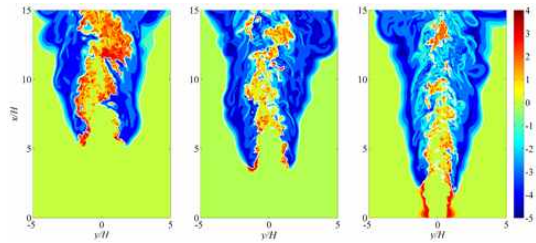

Figure 2. Isocontours of $\mathrm{sign}(\lambda_e)\times\log_{10}(\max(1,|Da_c|))$ for Case L, M, and H (from left to right). White lines denote th flamebase with $Da_c = 1$.

Figure 2 shows isocontour of Da_c in logscale for the cases. Note that a large positive Da_c in red indicates that the CEM dominates the mixing process such that the mixture is auto-igniting. A large negative Da_c in blue, however, indicates fast reacting post-ignition mixture such that its overall reaction progress can be limited by the slower local transport process. As such, the dark blue regions in Fig. 2 contain diffusion flame kernels. It is also readily observed that for Case H, there exist two strips of auto-igniting mixtures (red) upstream of the flamebase, leading to ignited mixtures (blue). This result verifies that the stabilization mechanism of Case H is auto-ignition. In Cases L and M, however, large positive Da_c occurs only at narrow regions right upstream of the flamebase, which corrspond to the preheated zone of a premixed flame. This result verifies that turbulent lifted flames for Cases L and M are mainly stabilized by flame propagation whereas the stabiliztion of the lifted flame for Case H is primarily attributed to auto-ignition of fuel-lean mixtures upstream of the flamebase.

The physicochemical characteristics of the flames are further investigated using the explosion index (EI) and participation index (PI), which represent the contribution of variables and reactions to CEM, respectively. The EI and PI vectors are defined as [5,6]:

$$\mathbf{EI} = \frac{|\mathbf{a}_e \otimes \mathbf{b}_e^T|}{\sum(|\mathbf{a}_e \otimes \mathbf{b}_e^T|)'}, \quad \mathbf{PI} = \frac{|\mathbf{b}_e \cdot \mathbf{S} \otimes \mathbf{R}|}{sum(|(\mathbf{b}_e \cdot \mathbf{S}) \otimes \mathbf{R}|)'}.$$

Figure 3 shows EI-weighted color-mixing contours of important variables to the CEM. In

Point	Location	EI (value, variable)	PI (value, variable)
1	x=-4.03H y=13.18H	0.99, H_2	0.49, R3: OH + H_2 = H_2O + H 0.13, R9: H + O_2 + M = HO_2 + M
2	x=-2.61H y=9.24H	0.40, O 0.27, H	0.69, R9: H + O_2 + M = HO_2 + M 0.14, R8: H + OH + M = H_2O + M
3	x=-1.71H y=6.90H	0.56, H 0.19, O2	0.70, R8: H + OH + M = H_2O + M
4	x=-1.81H y=5.34H	0.49, H2 0.47, T	0.49, R1: H + O_2 = O + OH 0.47, R9: H + O_2 + M = HO_2 + M
5	x=2.01H y=6.968H	0.37, H 0.28, H2	0.67, R9: H + O_2 + M = HO_2 + M 0.18, R8: H + OH + M = H_2O + M
6	x=1.05H y=12.48H	0.84, T	0.34, R11:HO_2 + H = OH + OH 0.19, R3: OH + H_2 = H_2O + H
7	x=-1.26H y=3.33H	0.87, T	0.13, R9: H + O_2 + M = HO_2 + M 0.38, R1: H + O_2 = O + OH
8	x=-1.47H y=2.13H	0.53, T 0.41, H2	0.50, R9: H + O_2 + M = HO_2 + M 0.50, R1: H + O_2 = O + OH
9	x=-1.23H y=2.04H	0.69, T 0.15, H2	0.48, R9: H + O_2 + M = HO_2 + M 0.47, R1: H + O_2 = O + OH
10	x=-0.93H y=0.54H	0.80, O	0.40, R9: H + O_2 + M = HO_2 + M 0.40, R1: H + O_2 = O + OH

Table 1. EI and PI values at selected points

addition, the variables and reactions with large EI and PI values at ten different locations are listed in Table 1. For all cases, temperture is found to be the most important variable right upstream of the flamebase. This is because temperaure becomes critical to a CEM in the preheated zone of premixed flame. Unlike Cases L and M, however, O and OH radicals are found to be important in the auto-igniting layers that can stabilize the lifted flame in Case H. In addition, two important reactions that control the auto-igniting layer are R1 and R9. This is because R1 and R9 are two competing reactions determining the 2nd explosion limit of H_2/O_2 mixture. It is also of interest to note that even in the preheated zone of Case L & M, and thermal ignition layer of Case H where temperature governs the CEM, R1 and R9 are also found to be the two most important reactions to the CEM. It is primarily because R9 is one of the major heat release reactions and R1 is the major endothermic reaction in both premixed and non-premixed H_2/air flames.

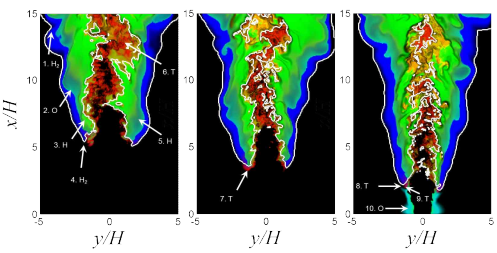

Figure 3 EI-weighted color-mixing contours of temperature (red), H_2 (blue), H (green), O (cyan), and O2 (yellow) for Cases L, M, and H. White lines denote the flamebase with Da_c =1.

In the lean mixtures of the lifted flames, H_2 becomes important to the CEM; however, in the rich mixtures of the flames, H becomes critical to rich premixed flame. From PI analysis (see Table 1), it is readily observed that in the lean mixures (Point 1), two major heat release reactions, R3 and R9 are identified as the most important reactions to the CEM. In the rich mixtures (Points 3 and 5), however, R8 and R9 are found critical to the CEM. It is also of importance to note that near the stoichiometric mixtures (Point 2), O and H are important EI species and R9 & R8 are the critical PI reactions.

Figure 4 shows the selective PI of R1 to

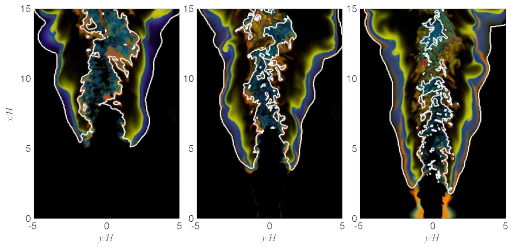

Figure 4 PI-weighted color-mixing contours of R1 (red), R2 (green), R3 (blue), R9 (yellow), and R10 (cyan) for Cases L, M, and H. White lines denote the flamebase with Da_c =1.

R10 of each case. PI of R10 (HO_2 + H = H_2 + O_2) forks at the upstream of flame base for Cases M and H, although its value is relatively small in Case M. A hook shaped PI for R9 appears occasionally at the right upstream of flamebase in Case M, while it sticks everytime on the flame base for case H.

R1, R2 (O + H_2 = H + OH) and R3 are the important chain branching reactions on flame propagation [8]. The shape of PI for R1 and R3 near downstream of flamebase exhibits nearly the same for both Cases L and M. The only difference is that in Case M, PI of R1 sometimes appears near downstream of white solid Da_c line like Case H where PI of R1 is always important immediately downstream of flamebase.

Case M have the characteristics of both flame propagation and auto-ignition near flamebase from a point of view of the behavior of PI. It can be conjectured that the stabilization mechanism for Case M is a mixed mode of auto-ignition and flame propagation in a qualitative manner.

The characteristics of stabilization mechanism and flame structure of turbulent lifted hydrogen jet flames in heated coflow at three temperatures of 750, 850 and 950 K near auto-ignition limit were investigated with a detailed H_2/O_2 mechanism. Overall flame structure and chemical explosive mode analyses revealed that auto-ignition is the main stabilization mechanism of the lifted jet flame for Case H and flame propagation is the main stabilization mechanism for Case L. The mixed mode of auto-ignition and flame propagation is found to be the main stabilization mechanisms for Case M from qualitative PI analysis. For all cases, T and H_2 are important variables in the preheated zone and thermal ignition layer upstream of the flamebase, where R1 and R9 are found the most importance reactions to the CEM.

Acknowledgements

This research was supported by the Basic Science Research Program (NRF-2015R1A2A2A01007378) and the Space Core Technology Development Program (NRF-2015M1A3A3A02027319) through the National Research Foundation of Korea (NRF) funded by the Ministry of Science, ICT & Future Planning.

References

[1] C. S. Yoo, E. S. Richardson, R. Sankaran, J. H. Chen, Proc. Combust. Inst. 33, 2011, pp 1619-1627.
[2] J. Li, Z. Zhao, A. Kazakov, F. L. Dryer, Int. J. Chem. Kinet. 36, 2004, pp 566-575.
[3] C. S. Yoo, Y. Wang, A. Trouvé, H. G. Im, Combust. Theory Modelling 9, 2005, pp 617-646.
[4] C. S. Yoo, H. G. Im, Combust. Theory Modelling 11, 2007, pp 259-286.
[5] T. Lu, C. S. Yoo, J. H. Chen, C. K. Law, J. Fluid Mech. 652, 2010, pp 45-64.
[6] Z. Luo, C. S. Yoo, E. S. Richardson, J. H. Chen, C. K. Law, Combust. Flame 159, 2012, pp 265-274.
[7] R. Shan, C. S. Yoo, J. H. Chen, T. Lu, Combust. Flame 159, 2012, pp 3119-3127.
[8] N. M. Marinov, C. K. Wcstbrook, W. J. Pitz, Transport phenomena in combustion 1, 1996, pp 118-129